Probing many-particle correlations in semiconductor quantum wells using double-quantum-coherence signals

Lijun Yang and Shaul Mukamel
Chemistry department, University of California, Irvine, California, 92697-2025, United States

ABSTRACT

Multidimensional analysis of coherent signals is commonly used in nuclear magnetic resonance to study correlations among spins. These techniques were recently extended to the femtosecond regime and applied to chemical, biological and semiconductor systems. In this work, we apply a two-dimensional correlation spectroscopy technique which employs double-quantum-coherence to investigate many-body effects in a semiconductor quantum well. The signal is detected along the direction $k_1+ k_2- k_3$, where k_1, k_2 and k_3 are the pulse wave vectors in chronological order. We show that this signal is particularly sensitive to many-body correlations which are missed by time-dependent Hartree-Fock approximation. The correlation energy of two-exciton can be probed with a very high resolution arising from a two-dimensional correlation spectrum, where two-exciton couplings spread the cross peaks along both axes of the 2D spectrum to create a characteristic highly resolved pattern. This level of detail is not available from conventional one-dimensional four-wave mixing or other two-dimensional correlation spectroscopy signals such as the photo echo ($-k_1+ k_2+ k_3$).

Keywords: double-quantum-coherence, many-particle correlation, two-dimensional correlation spectroscopy, ultrafast spectroscopy, semiconductor quantum wells.

1. INTRODUCTION

The coherent ultrafast response and many-body correlations in semiconductor heterostructures have been studied extensively in the past two decades [1-9]. Nonlinear four-wave mixing (FWM) experiments have long been known to provide direct probes for many-body effects in the ultrafast dynamics of excitons in semiconductor quantum wells. FWM signals are commonly displayed as a function of a single (time or frequency) variable, and hence provide a one-dimensional (1D) projection of the microscopic information. 1D spectra are hard to interpret in systems with many congested energy levels. The spectroscopic signatures of complex many-body dynamics projected on a 1D spectral plot strongly overlap and may not be easily identified within the observation window. This is particularly true for large semiconductor structures that contain many bound exciton states and continuum states. Moreover, due to various dephasing and relaxation mechanisms, the coherent response usually persists only on picosecond time scale. Thus, signatures of complex many-body dynamics may not be easily identified. For example, when 1D techniques are employed in GaAs III-V semiconductor quantum wells, it is difficult to pinpoint the signatures of two-excitons due to the small (1 to 2 meV) two-exciton correlation energies, i.e., biexciton binding energy and unbound two-exciton scattering energy. Two-exciton effects can be easily masked by homogeneous and inhomogeneous line broadening. When both light-hole (LH) and heavy-hole (HH) excitons and their interactions are taken into account, the situation becomes even more complicated since there are different types of two-excitons such as LH, HH and mixed two-excitons. Resolving this is hard even in II-VI semiconductor QWs, where the two-exciton interaction energies are much larger (from several to several tens of meV[10].

Multi-dimensional spectroscopy [11-13] in which the optical response is recorded and displayed versus several arguments, can overcome these limitations by separating the signatures of different pathways of the density matrix, known as Liouville space pathways[14]. Because different pathways are usually connected with specific couplings, one can resolve different coherences and many-body interactions by focusing on different peaks in multi-dimensional correlation plots. Visible and infrared 2D Correlation Spectroscopy (2DCS) is a femtosecond analogue of multi-dimensional nuclear magnetic resonance (NMR)[15-16] that has been shown to be very powerful for probing the

ljyang100@gmail.com; smukamel@uci.edu.

Ultrafast Phenomena in Semiconductors and Nanostructure Materials XIV, edited by Jin-Joo Song, Kong-Thon Tsen, Markus Betz, Abdulhakem Y. Elezzabi, Proc. of SPIE Vol. 7600, 76001G · © 2010 SPIE · CCC code: 0277-786X/10/$18 · doi: 10.1117/12.840993

structure and dynamics in chemical and biological systems[17-21]. These techniques can reveal the coupling strengths of elementary quasiparticle excitations through cross-peaks. After several attempts[22-26] to go beyond 1D techniques in semiconductors, the first experimental implementation of 2DCS to investigate the many-body Coulomb interactions among LH and heavy-hole HH excitons in semiconductors has been reported recently[27-28]. In this work, we present the basic principles of 2DCS of semiconductor quantum wells [29] and apply a specific 2DCS technique involving double-quantum-coherence to probe the exciton correlation energy [30-31] in semiconductor quantum wells with high resolution.

2. BASIC PRINCIPLES OF 2DCS

In 2DCS, three ultrashort laser pulses generate a signal which is heterodyne-detected by a fourth pulse in a chosen phase-matching direction, as shown in Figure 1. Three time delays t_1, t_2 and t_3 can be controlled between the four pulses, k_1, k_2 and k_3 and k_4. In an excitonic model, the possible phase-matching directions, $-k_1+k_2+k_3$, $-k_1+k_2+k_3$ and $-k_1+k_2+k_3$, represent three techniques referred to as S_I, S_{II} and S_{III} respectively [11,31]. The time-domain nonlinear signal, $S(t_1, t_2, t_3)$, is given by combinations of multi-time correlation functions which depend on the time t_1, t_2 and t_3. The 2DCS signal is displayed in the frequency-domain by a Fourier transform of $S(t_1, t_2, t_3)$ with respect to two time delays while holding the third fixed, i.e.,

$$\mathrm{S}\left(t_3,t_2,t_1\right)\rightarrow\begin{cases}\mathrm{S}\left(t_3,\Omega_2,\Omega_1\right)\\ \mathrm{S}\left(\Omega_3,t_2,\Omega_1\right),\\ \mathrm{S}\left(\Omega_3,\Omega_2,t_1\right)\end{cases}$$

where $\Omega_3,\Omega_2,\Omega_1$ are the Fourier conjugate frequencies corresponding to t_3, t_2, and t_1 respectively.

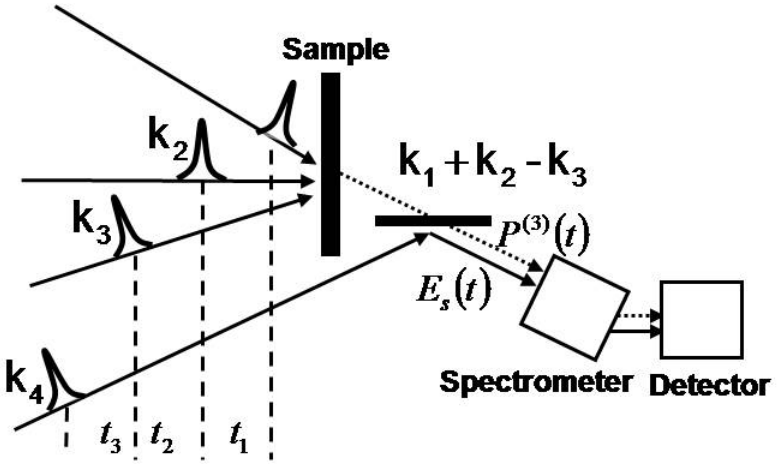

Figure 1. Schematic experimental setup for 2DCS.

The 2D spectrum provides a panoramic view with a much higher resolution not available in 1D four-wave-mixing (FWM) techniques. Strict time ordering among different pulses further simplifies the spectra. Note that three time delays t_1, t_2 and t_3 are all positive in contrast to the conventional FWM where there is no fixed time ordering among the pulses and their delays can be either positive or negative. With the time ordering among the pulses and detection of the signal along specific phase-matching directions in 2DCS, quantum pathways involved in the third-order response can be separated. For example, within the rotating wave approximation for resonant excitations, all quantum pathways involved can be separated into three groups, each corresponds to a particular direction, as shown in Figure 2 [11, 14]. These pathways are represented by the double-sided Feynman, where e and f represent respectively single-exciton and two-

exciton manifolds and g represents ground state (exciton level scheme is shown on top right of Figure 2). The rules of these diagrams were given in Ref. [14].

The time-ordering of the pulses and directional detection in 2DCS thus help identify which quantum pathways are involved in a particular technique. For example, the photo-echo signal corresponds to the S_I technique. FWM experiments involving double-quantum-coherence, however, correspond to S_{III} technique. The widely applied pump-probe experiments, are most easy to implement but hard to interpret since they are the combination of S_I and S_{II} due to the lack of time ordering among the pump and probe pulses. Moreover, S_I, S_{II} and S_{III} techniques provide complementary information. The focus of this paper is on the probing of two-exciton correlation energy and thus the best choice is S_{III} which involves double-quantum-coherence during t_2. This technique is not suitable for studying population transport because population is never created. Incoherent population transfer can be studied using S_I or S_{II} where population is prepared during the time delay t_2.

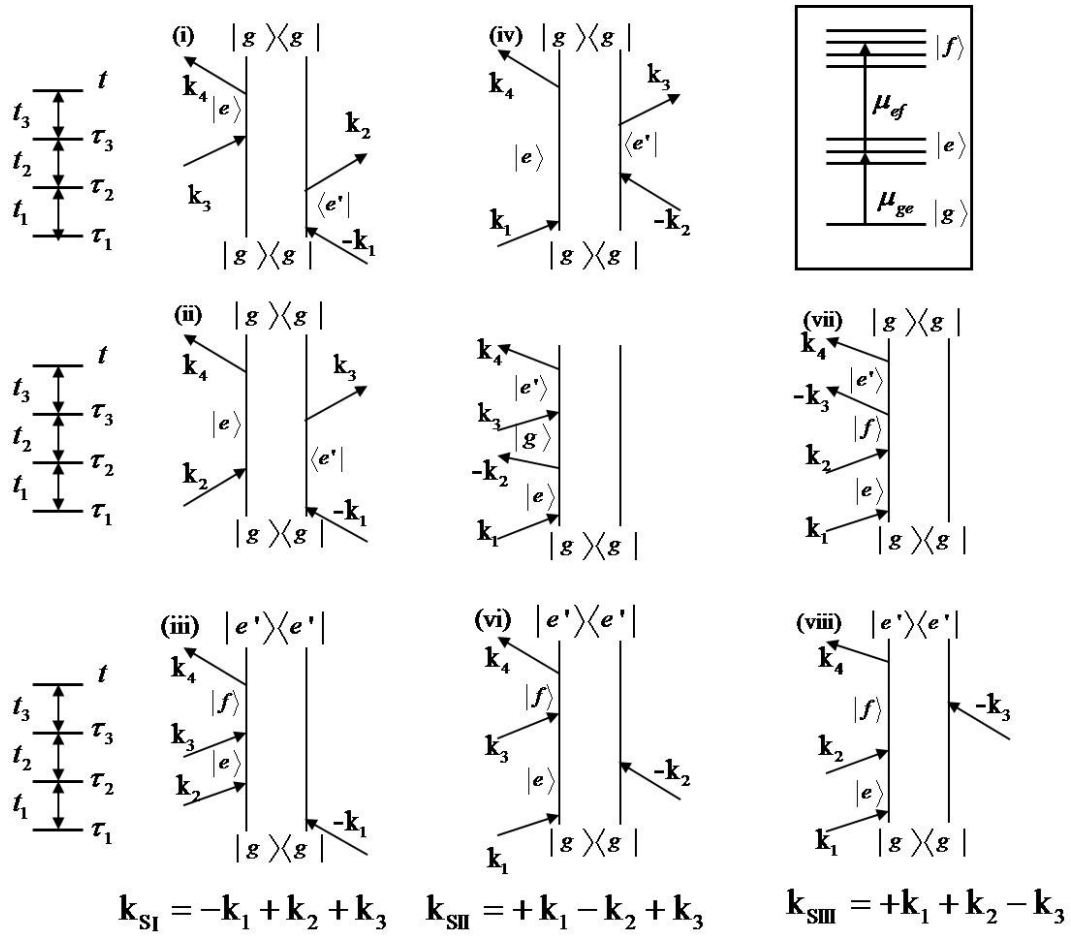

Figure 2. Feynman diagrams for the three possible coherent 2D spectroscopic techniques.

3. HEAVY-HOLE EXCITONS AND TWO-EXCITONS IN GAAS QUANTUM WELLS

We study the correlation energy of two-excitons, we next consider only the correlation energy among heavy-hole (HH) excitons in semiconductor quantum wells using the S_{III} technique. We first present a qualitative study of the 2D spectrum with double-sided Feynman diagrams. In semiconductor quantum wells, two single excitons can form three types of two-excitons: unbound, bare and bound two-excitons, with respectively the energy of f_1, f_2 and f_3, as

schematically shown in the top left of Figure 3. R and L in Figure 3 indicate respectively right and left circularly polarized photons. With this level scheme, the two Feynman diagrams in Figure 2 for S_{III} (diagrams vii and viii) reduce to the two diagrams on the top right of Figure 3, where indices e' and e are collapsed into a single index e due to the existence of only one type of excitons (HH). However, the two-exciton state, f can still assume three possible values f_1, f_2 and f_3.

To simplify our discussion, we assume that only bound two-excitons exist ($f = f_3$) and thus the two diagrams on the top right further simplify to the two diagrams on the bottom left. We now use this simplified Feynman diagrams to predict the schematic 2D spectrum. We investigate the S_{III} signals in the (Ω_3, Ω_2) plane. In the time domain, we thus investigate the resonance during t_3 and t_2. From diagram (vii) in the bottom left, we see the resonance energy during during t_3 and t_2 are respectively e and $f_3 = 2e\text{-}\Delta_b$, where Δ_b is the correlation energy of bound two-excitons. Thus in the (Ω_3, Ω_2) plane, we obtain a signal at (e, $2e\text{-}\Delta_b$). This contribution is denoted by a solid square and is illustrated in the 2D spectrum on the bottom right of Figure 3. Using the same analysis but for diagram (viii) in the bottom left, we obtain the signal at $(\Omega_3, \Omega_2) = (e\text{-}\Delta_b, 2e\text{-}\Delta_b)$, denoted by a solid square.

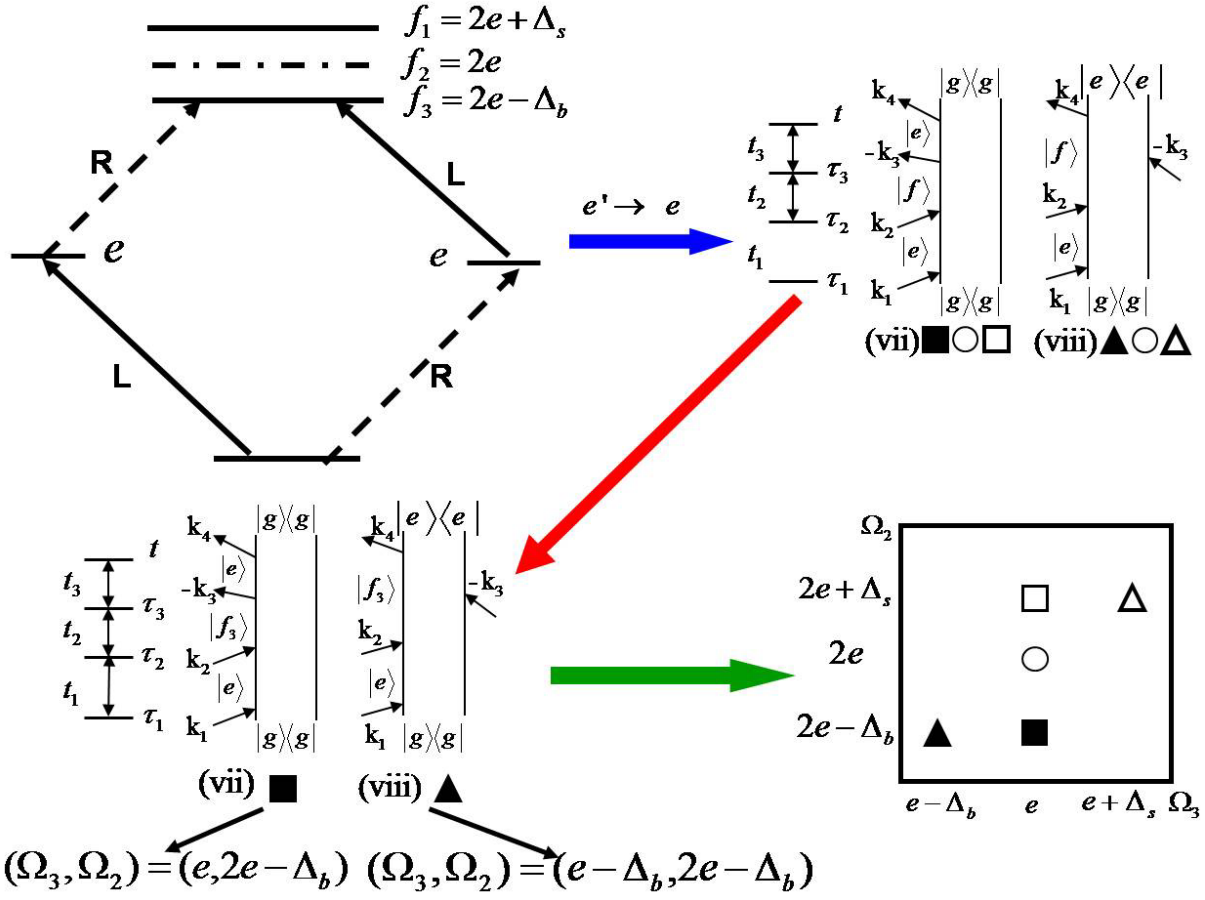

Figure 3. Schematic 2D spectrum derived from S_{III} Feynman diagrams for HH excitons in semiconductor quantum wells.

Incorporating the bare and unbound two-excitons, $f = f_1$ and f_2, we obtain another two sets of Feynman diagrams. These contributions are denoted by the open square and triangle for unbound two-excitons, and open circle for bare two-excitons, as shown in Figure 3. Feynman diagram analysis allows to predict the schematic 2D spectrum without detailed calculations. This will help to assign the key features of calculated 2DCS signals presented below.

4. NUMERICAL SIMULATIONS

2DCS signals are usually calculated using nonlinear response functions by summing over the relevant eigenstates of a system [14]. The exciton eigenstates of many-body systems such as quantum wells are too expensive to calculate. Therefore, alternative quasi-particle techniques are applied to calculate nonlinear response signals. These include the Nonlinear Excitonic Equations (NEE) [32-35] or the Dynamics Controlled Truncation (DCT) formalism [4] to account for the many-body interactions beyond the time-dependent Hartree-Fock (TDHF) level. To close the infinite hierarchy of dynamical variables, the equations of motion are truncated according to the desired order of the laser field. However, calculating the 2DCS of semiconductor quantum wells still requires an intensive numerical effort. To make these calculations tractable, we shall use a multi-band one-dimensional tight-binding model [8] to describe the excitons and two-excitons of a single quantum well. This model reproduces many spectroscopic observables in quantum-wells such as the signs of energy shifts, bleaching and induced absorption and often even their relative strengths, and the dependence on the polarization directions of the incident pulses. Details of the calculation can be found in Refs. [29,31]

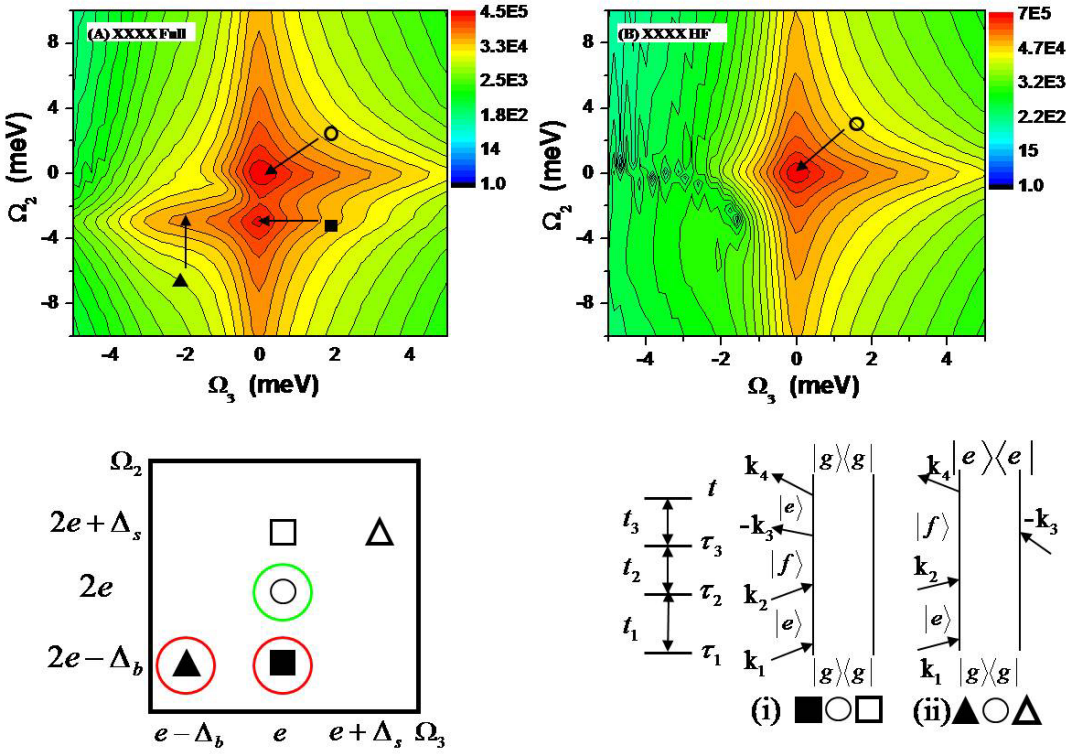

Figure 4. (Top) The 2D spectra simulated with full calculation (Panel A) and within time-dependent Hartree-Fock approximation (Panel B). (Bottom) Schematic 2D spectrum and the corresponding Feynman diagrams. The laser pulses are tuned to the red of exciton energy in the calculation.

In Figure 4, we present the simulated 2D S_{III} spectra. Using the same parameters of Ref. [36], we set the dephasing times for excitons and two-excitons to be 2ps and 1ps respectively. All spectra are calculated with Gaussian pulses. The frequency origin in all panels is set to e for Ω_3 and 2e for Ω_2, where e is the single HH exciton energy (~ 1520 meV). All peaks or shoulders are assigned using the symbols given in Figure 3. Panel (A) attempts to probe two-exciton

binding energy (TBE) and hence the pulse parameters are chosen such that red shifted two-excitons are selectively excited. Due to the specific tuning of pulse center frequency and narrow bandwidth, only three of the five peaks in the schematic 2D spectrum are shown, as indicated by three symbols: solid square, triangle and open circle. The corresponding schematic 2D spectrum and the Feynman diagrams are also presented at the bottom of Figure 4.

In panel (A), circles and solid squares are strong and well resolved along Ω_2, while solid squares and triangles are not resolved along Ω_3. This can be understood by examining the resonances. Along t_2, both S_{III} diagrams have only two-exciton to ground-state resonance (f-g) and thus Ω_2 provides a clean projection of the two-exciton correlation energy. However, along t_3, one diagram has exciton-ground-state resonance (e-g), and the other has two-exciton to ground-state resonance (f-e). These two resonances will be mixed in the total signal and thus reduce the resolution. This is particularly true when the two-exciton correlation energy is small and comparable to the exciton line width. From these arguments, we know that the Ω_2 value of the solid square gives the TBE (the separation of open circle and solid square). The TBE can thus be obtained from the well-resolved solid square in panel A. We thus circumvent the difficulty of probing TBE from the splitting between solid square and the unresolved solid triangle, which overlap with e-g and f-e resonances along Ω_3. Panel (B) is calculated by the TDHF approximation which neglects two-excitons correlations. As expected, features related to red shifted two-excitons such as the solid square and triangle, vanish.

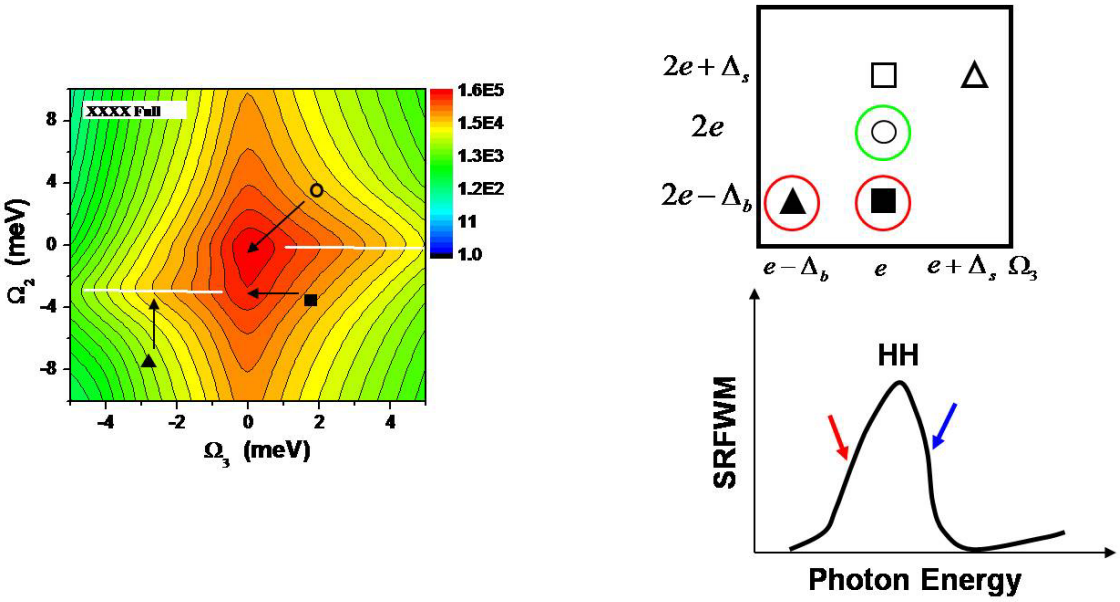

Figure 5. (Left) Calculated 2D spectrum with fast dephasing times). (Right)

Schematic 2D spectrum and spectrally resolved FWM signal.

Thanks to the panoramic view offered by the 2D spectrum, the TBE may be extracted even it is comparable or smaller than the single-exciton line broadening. Figure 5 shows the 2D spectrum calculated with faster dephasing times, 1.0ps/0.5ps, for exciton/two-excitons. Under this situation, the two peaks denoted by the circle and solid square cannot be resolved even along the clean Ω_2 axis. However, it is still possible to obtain the TBE from the 'ridge' of the contour lines (two white lines). The TBE is given by the Ω_2 value of the bottom line. The reason leading to the identification of this white line is the coexistence of solid triangle and square in a 2D spectrum. Such resolution cannot be achieved by conventional 1D FWM techniques. For example, as schematically shown at the bottom right of Figure 5, although we can see a bump to the left of HH exciton in a spectrally resolved FWM signal (marked by a red arrow), we cannot resolve the TBE due to the large exciton broadening.

In Figure 6, the calculations of Figure 4 are repeated but with pulses tuned to the blue side [30] of single-exciton in order to resolve the two-exciton scattering energy (TSE), which arises from the interaction of two same-spin excitons.

We can obtain the blue-shifted TSE, from the open triangle (a shoulder but not a resolved peak) in panel A, even though we cannot resolve open square from two-exciton continuum along Ω_2. We obtain the TSE by the Ω_2 value of the peak denoted by the open triangle. In a 1D spectrally resolved FWM experiment, we cannot achieve such a resolution, as schematically shown in the bottom left of Figure 6, where we cannot resolve the TSE by a bump pointed by a blue arrow. Panel (B) repeats the calculation in panel (A) using the TDHF approximation. As expected, the higher-order correlation effects such as the open square and triangle in panel (A) are missing.

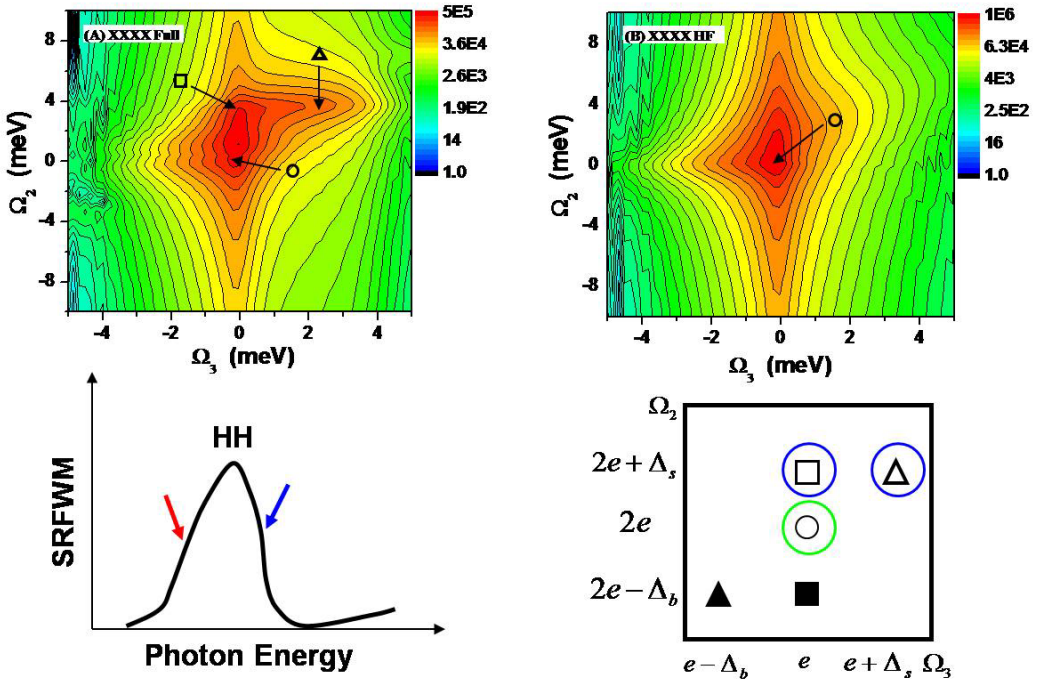

Figure 6. (Top). The 2D spectra simulated with full calculation (Panel A) and with time-dependent Hartree-Fock approximation (Panel B). (Bottom). Schematic 1D spectrally resolved FWM signal (left) and 2D spectrum (right). The laser pulses are tuned to the blue of exciton energy.

We demonstrate that a 2DCS technique, S_{III}, is intrinsically sensitive to two-exciton correlations and can distinguish between different species of excitons and two-excitons in photo-excited semiconductors by spreading them along two axes. Combining the information from different Liouville space pathways, this technique can accurately retrieve two-exciton binding energy even when it is smaller than exciton line broadening. We further report an unambiguous signature of correlated unbound two-excitons lying underneath the two-exciton continuum.

In summary, we demonstrate that 2DCS with double-quantum-coherences gives much higher resolution to exciton correlation energies than other 2DCS and 1D FWM techniques. This is due to the fact that the TBE-related contribution (solid square) always has an associated feature (solid triangle) to the red, and the TSE related contribution (open square) always has an associative feature (open triangle) to the blue, as qualitatively described in Figure. 3. Moreover, the solid square and triangle (open square and triangle) always appear in pairs and thus we can easily obtain accurate TBE(TSE) by identifying both features, even when line broadening is large. For example, in Figure 5, the much weaker solid triangle plays a crucial role in identifying the solid square. Similarly, in Figure 6, we cannot identify the open square without the help of the open triangle. Thus it is impossible to resolve the signature of blue-shifted two-excitons (unresolved open square and triangle) in Figure 6 with conventional 1D FWM where the signature will either be covered by the two-exciton continuum along Ω_2 or along Ω_3 by the broadening of the much stronger single-exciton peak, the circle. This cannot be obtained from any other 2DCS techniques where two-excitons show up along a single axis (Ω_3 but not Ω_2). However, with double-quantum-coherence 2DCS, we can easily obtain very accurate TSE, even though the open square and triangle are weak and may not be resolved along any single axis.

ACKNOWLEDGMENTS

This research was supported by the National Institutes of Health (Grant GM59230), National Science Foundation (Grant CHE-0745892), and the Chemical Sciences, Geosciences and Biosciences Division, Office of Basic Energy Sciences, Office of Science, U.S. Department of Energy.

REFERENCES

[1] H. Haug and S. W. Koch, Electronic Properties of Semiconductors, fourth Edition, (World Scientific, 2004).
[2] J. Shah, Ultrafast Spectroscopy of Semiconductors and Semiconductor Nanostructures, second enlarged edition, (Springer, 1999).
[3] D. S. Chemla and J. Shah, "Many-body and correlation effects in semiconductors", Nature 411, 549 (2001).
[4] V. M. Axt and S. Mukamel, "Nonlinear Optics of Semiconductor and Molecular Nanostructures; A Common Perspective," Rev. Mod. Phys. 70, 145 (1998).
[5] F. Rossi and T. Kuhn, "Theory of ultrafast phenomena in photoexcited semiconductors," Rev. of Mod. Phys. 74, 895 (2002).
[6] N. H. Kwong and R. Binder, "Green's function approach to the dynamics-controlled truncation formalism: Derivation of the $\chi^{(3)}$ equations of motion," Phys. Rev. B 61, 8341 (2000).
[7] W. Schäfer, D. S. Kim, J. Shah, T. C. Damen, J. E. Cunningham, K. W. Goossen, L. N. Pfeiffer, and K. Köhler, "Femtosecond coherent fields induced by many-particle correlations in transient four-wave mixing," Phys. Rev. B 53, 16429 (1996).
[8] T. Meier, P. Thomas, and S. W. Koch, Coherent Semiconductor Optics : From Basic Concepts to Nanostructure Applications , (Springer, 2007).
[9] H. Wang, K. B. Ferrio, D. G. Steel, Y. Z. Hu, R. Binder, and S. W. Koch, "Transient nonlinear optical response from excitation induced dephasing in GaAs," Phys. Rev. Lett. 71, 1261 (1993).
[10] H. P. Wagner, W. Langbein and J. M. Hvam, "Mixed biexcitons in single quantum wells," Phys. Rev. B 59, 4584 (1999).
[11] S. Mukamel, "Multidimensional Femtosecond Correlation Spectroscopies of Electronic and Vibrational Excitations," Ann. Rev. Phys. Chem. 51, 691-729 (2000).
[12] V. Chernyak, W. M. Zhang and S. Mukamel, "Multidimensional Femtosecond Spectroscopies of Molecular Aggregates and Semiconductor Nanostructures; The Nonlinear Exciton Equations," J. Chem. Phys. 109, 9587 (1998).
[13] S. Mukamel and D. Abramavicius, "Many-Body Approaches For Simulating Coherent Nonlinear Spectroscopies of Electronic and Vibrational Excitons," Chem. Rev., 104, 2073-2098 (2004).
[14] S. Mukamel, Principles of Nonlinear Optical Spectroscopy, (Oxford University Press, New York, Paperback edition (1995)).
[15] Ernst R. R., Bodenhausen G., Wokaun A. 1987. Principles of Nuclear Magnetic Resonance in One and Two Dimensions. Oxford, UK: Clarendon.
[16] Evans J. N., 1995. Biomolecular NMR Spectroscopy, New York: Oxford Univ. Press.
[17] D. Abramavicius and S. Mukamel, "Coherent third-order spectroscopic probes of molecular chirality," J. Chem. Phys., 122, 134305 (2005).
[18] J. Zheng, K. Kwak, J. Asbury, X. Chen, I. Piletic, and M. D. Fayer, "Ultrafast Dynamics of Solute-Solvent omplexation Observed at Thermal Equilibrium in Real Time," Science 309, 1338-1343 (2005).
[19] Ch. Kolano, J. Helbing, M. Kozinski, W. Sander, P. Hamm. Nature 444, 469 - 472 (2006)
[20] T. Brixner, J. Stenger, H. M. Vaswani, M. Cho, R. E. Blankenship and G. R. Fleming, "Two-dimensional spectroscopy of electronic couplings in photosynthesis," Nature 434, 625-628 (2005).
[21] M. C. Asplund, M. T. Zanni, R. M. Hochstrasser, "Two-dimensional infrared spectroscopy of peptides by phase-controlled femtosecond vibrational photon echoes," Proc. Natl. Acad. Sci. USA 97, 8219 (2000).
[22] M. Koch, J. Feldmann, G. von Plessen, E. O. Göbel, P. Thomas and K. Köhler, "Quantum beats versus polarization interference: An experimental distinction," Phys. Rev. Lett. 69, 3631 (1996).
[23] V. G. Lyssenko, J. Erland, I. Balslev, K.-H. Pantke, B. S. Razbirin, and J. M. Hvam, "Nature of nonlinear four-wave-mixing beats in semiconductors," Phys. Rev. B 48, 5720 (1993).

[24] S. T. Cundiff, M. Koch, W. H. Knox, J. Shah and W. Stolz, "Optical Coherence in Semiconductors: Strong Emission Mediated by Nondegenerate Interactions," Phys. Rev. Lett. 77, 1107 (1996).
[25] A. Euteneuer, E. Finger, M. Hofmann, W. Stolz, T. Meier, P. Thomas, S. W. Koch, W. W. Rühle, R. Hey and K. Ploog, "Coherent Excitation Spectroscopy on Inhomogeneous Exciton Ensembles," Phys. Rev. Letts. 83, 2073 (1999).
[26] E. Finger, S. Kraft, M. Hofmann, T. Meier, S.W. Koch, W. Stolz, W.W. Rühle, and A. Wieck, "Coulomb Correlations and Biexciton Signatures in Coherent Excitation Spectroscopy of Semiconductor Quantum Wells," phys. stat. sol. (b) 234 (1), 424 (2002).
[27] Xiaoqin Li, Tianhao Zhang, Camelia N. Borca, and Steven T. Cundiff, " Many-body interactions in semiconductor quantum wells probed by optical two-dimensional Fourier transform spectroscopy," Phys. Rev. Lett. 96, 57406 (2006).
[28] C. N. Borca, T. Zhang, X. Li and S. T. Cundiff, "Optical two-dimensional Fourier transform spectroscopy of semiconductors" Chem. Phys. Lett. 416, 311 (2005).
[29] L. Yang, I. Schweigert, S. Cundiff and S. Mukamel, "Two-Dimensional Optical Spectroscopy of Excitons in Semiconductor Quantum Wells: Liouville-Space Pathways Analysis", Phys. Rev. B 75, 125302 (2007).
[30] L. Yang and S. Mukamel, "Two-Dimensional Correlation Spectroscopy of Two-Exciton Resonances", Phys. Rev. Lett., 100, 057402 (2008).
[31] L. Yang and S. Mukamel, "Revealing exciton-exciton couplings in semiconductors using multidimensional four-wave mixing signals," Phys. Rev. B., 77, 075335 (2008).
[32] F. C. Spano and S. Mukamel, Phys. Rev. Letts. 66, 1197 (1991).
[33] F. C. Spano and S. Mukamel, "Excitons in Confined Geometries: Size Scaling of Nonlinear Susceptibilities," J. Chem. Phys. 95, 7526 (1991).
[34] J. A. Leegwater and S. Mukamel, "Exciton Scattering Mechanism for Enhanced Nonlinear Response of Molecular Nanostructures," Phys. Rev. A 46, 452 (1992).
[35] S. Mukamel, Molecular Nonlinear Optics, J. Zyss, Editor, Academic Press, New York, 1-46 (1994).
[36] S. Weiser, T. Meier, J. Möbius, A. Euteneuer, E. J. Mayer, W. Stolz, M. Hofmann, W. W. Rühle, P. Thomas, and S. W. Koch, "Disorder-induced dephasing in semiconductors," Phys. Rev. B 61, 13088 (2000).